ISEIS

Journal of Environmental Informatics 42(2) 143-157 (2023)

Journal of Environmental Informatics

www.iseis.org/jei

Differences in China Greening Characteristics and its Contribution to Global Greening

X. Zhang[1], D. H. Yan[1 *], T. L. Qin[1 *], C. H. Li[1], and H. Wang[1]

[1] *State Key Laboratory of Simulation and Regulation of Water Cycle in River Basin, China Institute of Water Resources and Hydropower Research, Beijing 100038, China*

Received 20 July 2022; revised 06 September 2022; accepted 22 December 2022; published online 15 September 2023

ABSTRACT. With the rapid emergence of the global greening phenomenon under remote sensing monitoring, the prevailing trend of phenomenon analysis and traceability research is self-evident. However, identifying characteristics is basic research of the greening phenomenon, which sometimes subverts research results. The choice of method may directly affect the difference in the greening-browning range, which is easily overlooked. At the same time, influenced by the regional vegetation state's basic value, the greening contribution's spatialization still needs to be further verified. Based on the enhanced vegetation index results at the global kilometer-grid scale, this research chose to use the maximum value composite and the simple average method to explore the differences in China's characteristic identification process initially. While paying attention to results and phenomena, scholars' attention to basic research needs further improvement. The results show that the widely used two groups of basic methods have shown noticeable differences in greening and browning, and are affected by human activities, climate, geographical environment, etc. And this directional error and the phenomenon of hasty generalization are the most easily ignored in much basic research. The vegetation information considering the inherent stock and changing flux has quantified the greening contribution between regions. China, Brazil, and India dominate global greening, and Canada significantly contributes to browning. Some regions must promote the greening trend of changing flux while maintaining the inherent stock advantage.

Keywords: greening rate and degree, greening contribution, partial correlation analysis, greening-browning boundary

1. Introduction

Remote sensing data monitoring shows that the trend of greening has gradually improved in recent decades, and the greening phenomenon in the region and even the whole world has been reported one after another, which has attracted the attention of all parties (Bogaert et al., 2002; Piao et al., 2020). Among them, traceability and identification of the driving factors have gradually become a hot spot in the greening phenomenon (Zhu et al., 2016; Parida et al., 2020; Maina et al., 2022). And it is more practical to imitate or promote the greening model, which may be one of the important reasons. However, the scientific identification of the greening phenomenon or greening characteristics, as the theoretical basis of the above research, may subvert the results of its driving factor analysis to a certain extent, which is also the most easily overlooked part of the current research.

The research area may not be the greening or browning as it appears. How to define greening? How to characterize the greening characteristics? More is reflected by the trend of regional vegetation greenness proxies (Yao et al., 2019), such as leaf area index (Forzieri et al., 2017), vegetation index (Huete et al., 2002; De Jong et al., 2011; Liu et al., 2015), vegetation production system (Zhang et al., 2008; Feng et al., 2021b), etc. Because vegetation growth is periodic and continuous, the trend research process of greenness proxies is usually carried out over a long period. Therefore, in integrating discrete information, we typically construct an index variable to replace or synergistically reflect the characteristics of statistical periods, such as maximum value composite (MVC) (Piao et al., 2011; Yuan et al., 2022), simple average method (SAM) (Propastin et al., 2008; Chen et al., 2021), and other methods. Among them, MVC and SAM have commonly used methods in EVI statistical analysis, which complement each other, and each has its advantages and disadvantages in evaluating greening. The feature sequence constructed based on the annual maximum can clearly describe the change degree of the extreme value within the year, the trend change is more drastic, and the spatial representation ability is more potent. However, because the data information is limited to the annual maximum, the degree of disturbance is higher. The feature sequence based on the SAM averages the information within the year, which contains much information and is less disturbed. It is easy to cause slight data differences and weak spatial representation ability. The actual situation of vegetation greenness is easy to be ignored due to the lack of reasonable judgment. Under different spatial scales

* Corresponding author. Tel.: +86-10-6878-1650; fax: +86-10-6841-2316.
E-mail address: yandh@iwhr.com (D. H. Yan).
E-mail address: qintl@iwhr.com (T. L. Qin).

ISSN: 1726-2135 print/1684-8799 online
 doi:10.3808/jei.202300502.

and underlying surface types, there are apparent differences in the greening characteristics of various methods. For example, in areas affected by human activities, primarily cultivated land, it is unreasonable that the decline of the maximum index is considered browning. This is more due to the adjustment of the planting system and crops. The change in multiple cropping reduces the maximum index and also increases the overall amount of annual information. Using the same index to characterize the greening characteristics is bound to be distorted. Considering only the dynamic information of vegetation, it is still necessary to classify and integrate different topography, land cover, and utilization methods.

At the same time, with the increasing attention to the global greening phenomenon, the differences between regions and their impact on global greening are significant (Chen et al., 2019; Cortés et al., 2021). However, it is difficult to compare the contribution of greening among regions in the process of spatial statistics. The regional vegetation state's basic value will affect global greening characteristics. Due to the influence of many factors such as statistical area and regional natural geographical environment, even if it does not show a trend of greening, the proportion of global greening with high basic value must be increased, and vice versa. Although the difference in basic values is essential, whether or not to greening and the rate of greening should also be regarded as one of the assessment indicators and should be reflected in different regions.

Driven by policies, China greening impact has attracted world-wide attention. Ecological restoration and protection are considered to have made remarkable contributions (Chen et al., 2019; Feng et al., 2021a), especially in the field of climate change. And objectively revealing the practice of China greening can support further actions to upgrade the construction of ecological civilization. There are significant spatial differences in vegetation characteristics in China. The revealing degree of a single index is open to question, the greening-browning phenomenon is still unclear, and there is no clear conclusion on the quantitative contribution of China to global greening. Therefore, this research aims to solve two critical scientific problems: (1) Exploring the spatio-temporal changing of dynamic vegetation information at different methods to discriminate directional errors and boundary problems caused by method differences from a more comprehensive and scientific group. (2) Considering the growth rate of greening and its differences, the contribution of different countries such as China to global greening is quantified by constructing the cumulant sequence of gaps, in order to improve the international community's awareness of the greening phenomenon, scientifically control and adapt to it.

2. Material and Methods

2.1. Basic Data Sources

Basic data mainly includes the digital elevation model, human footprint, land cover, vegetation index, etc. (Table 1). Due to the difference in spatial resolution, the statistical information of the grid background value is extracted after overlapping data, and there may be cases where adjacent data are similar. In this research, the scale factor has not been used for data conversion in the EVI processing (EVI valid range: −3,000 ~ 10,000, dimensionless data).

2.2. Evaluation Index and Method

2.2.1. Greening Rate

The greening rate belongs to the trend category, which is consistent with the concept of slope. Positive and negative changes are used to distinguish greening or browning, and the magnitude of the slope indicates the greening rate over a period. Therefore, this research uses the least square method to evaluate the greening rate of feature sequences represented by SAM and MVC, and the calculation formula is as follows:

$$slope = \frac{n \times \sum_{i=1}^{n} \left(i \times SS_i \right) - \sum_{i=1}^{n} i \times \sum_{i=1}^{n} SS_i}{n \times \sum_{i=1}^{n} i^2 - \left(\sum_{i=1}^{n} i \right)^2} \quad (1)$$

where SS_i indicates the annual change of feature sequence (i = 1, 2, …, n), and n is the total length of sequence. The feature sequence in this research refers to constructing 16-day discrete datasets in the source data into a feature sequence with an interval of years using MVC and SAM methods.

2.2.2. Greening Degree

Generally, the evaluation of a greening degree needs to have a reference state. Greening is an increase or decrease by a certain percentage relative to the reference state. Therefore, this research mainly introduces the concept of a relative gradient to discuss the greening degree, and the calculation formula is as follows:

$$RG = n \times slope \Big/ \sum_{i=1}^{n} SS_i \quad (2)$$

where $\Sigma SS_i / n$ (the average value of annual characteristic sequence) is taken as the reference state to evaluate the greening degree, in order to explore the contribution degree of greening rate to its average value.

2.3. Evaluation Method of Global Greening Contribution

Since regional greening or browning is an ongoing event, the influence of basic values and trend changes in greening must be regarded in assessing global greening contributions. The detailed evaluation procedures are provided in the subsections below.

2.3.1. Constructing the Cumulant Sequence of Gaps

The cumulant sequence of gaps in different regions or globally is constructed, and the calculation formula is as follows:

Table 1. Description and Sources of Basic Data

Name	Data description	Source	URL
MOD13A2	Global Enhanced Vegetation Index from 2000 to 2021, time resolution: 16 days, spatial resolution: 1 km × 1 km	NASA	https://lpdaac.usgs.gov/products/mod13a2v006/
GlobeLand30	Global Land Cover for 2010, spatial resolution: 30 m × 30 m	China	https://www.webmap.cn/main.do?method=index
STRM-DEM	Global Digital Elevation Model, spatial resolution: 90 m × 90 m	NASA	https://lpdaac.usgs.gov/products/srtmgl1v003/
Human Footprint	Global terrestrial Human Footprint maps for 2009, spatial resolution: 1 km × 1 km	Scientific Data	https://www.nature.com/articles/sdata201667

$$CSG = \sum_{i=2}^{n}\left(\sum_{c=1}^{c_{max}} Evi_{c,i} - \sum_{c=1}^{c_{max}} Evi_{c,1}\right) \tag{3}$$

where *Evi* indicates the basic value of the original EVI data. *c* indicates the amount of annual data available (c_{max} = 23, there are 23 remote sensing images in one year). $Evi_{c,1}$ indicates the EVI data within the first year (2001 in this research).

2.3.2. Cumulative Contribution Comparison Method Considering the Influence of Slope

Based on *CSG*, the *slope* of each region or globally is obtained by the least square method (Equation (3)). Considering the slope correction of each region, the cumulative contribution degree is re-evaluated, and the calculation formula is as follows:

$$\begin{cases} c\_CSG_j = CSG_j / CSG_{all} \times 100 \\ c\_slope_j = slope_j / slope_{all} \times 100 \end{cases} \tag{4}$$

where *c_CSG* and *c_slope* are the contribution degree of cumulant and slope respectively. *j* denotes different regions. *all* indicates the global scope. The influence of region on the overall change can be explained by positive and negative changes of *c_CSG*, while the increasing and decreasing trend of region is reflected by *c_slope*. When the changes are opposite, it is necessary to appropriately reduce the overall impact. Therefore, the calculation formula of regional slope correction coefficient (*AD*) and contribution degree (*C*) is constructed as follows:

$$AD_j = \begin{cases} c\_slope_i / c\_slope_{i-max}, \\ \qquad c\_CSG_i \ge 0; c\_slope_i \ge 0 \\ |c\_slope_i| / (c\_slope_{i-max} - c\_slope_i), \\ \qquad c\_CSG_i \ge 0; c\_slope_i < 0 \\ -c\_slope_i / |c\_slope_{i-min} - c\_slope_i|, \\ \qquad c\_CSG_i < 0; c\_slope_i \ge 0 \end{cases} \tag{5}$$

$$C_j = c\_CSG_j \times AD_j \tag{6}$$

3. Results

3.1. Preliminary Study of Vegetation Cover

According to MVC and SAM methods, the spatial distribution characteristics of fractional vegetation cover in China from 2001 to 2021 are identified (Figures 1a and 1b). The continuity and fragmentation of spatial distribution can fully reflect that the fluctuation of MVC is more prominent. SAM will homogenize the information within the year, and the change in vegetation cover is slight. For example, although MVC shows a higher vegetation cover, the northwest in China still belongs to the form of low vegetation cover. Northeast and Southwest in China are worthy of attention, and some show a high cover trend similar to that of the South in MVC identification. Still, the spatial continuity of patches changes obviously after averaging and grading. After comparison, it is evident that the effect presented by SAM is closer to the actual well-known situation. The unified treatment with MVC or SAM is often regarded as a pretreatment method for greening analysis. However, it is still one-sided in the scientific identification of regional greening characteristics. Therefore, it is necessary to initially explore this differentiation from the research between different methods and judge the greening characteristics on a more comprehensive and scientific level.

3.2. Difference of Greening Rate

It is historicity that large-scale greening has been observed across China in recent decades. According to two groups of indicators (Figures 2a and 2b), the overall character of vegetation in China is greening (Greening rate based on SAM: 1.37%/10yr. Greening rate based on MVC: 2.09%/10yr). The proportion of greening area in China is significant, but the trend of MVC changes more sharply in extreme cases (the red box of Figure 3a). Because of the particularity shown by the above MVC method, the corresponding units in Figure 3a are extracted with the EVI greening rate greater than 50/yr and the continuous area exceeding 100 km^2 as constraints, which are primarily located in northeastern (region 3), central (region 4), and northwestern (region 5) in China. Further, the corresponding units in Figure 3a are extracted with the EVI greening rate less than −10/yr and the continuous area exceeding 100 km^2 as constraints. And the region's location is mainly in the Huang-Huai-Hai Plain. Among them, region 1 represents a sharp contrast between greening (Presented by SAM) and browning (Presented by MVC), and region 2 represents the region with similar trends of the two methods. Regions 3, 4, and 5 indicate the characteristic regions where the greening rate of EVI is greater than 50/yr (Feng et al., 2021a). The annual variation of EVI in this region is unimodal (Using a logistic model to calculate the phenological characteristics of EVI after SG filtering (Zhang et al., 2003)),

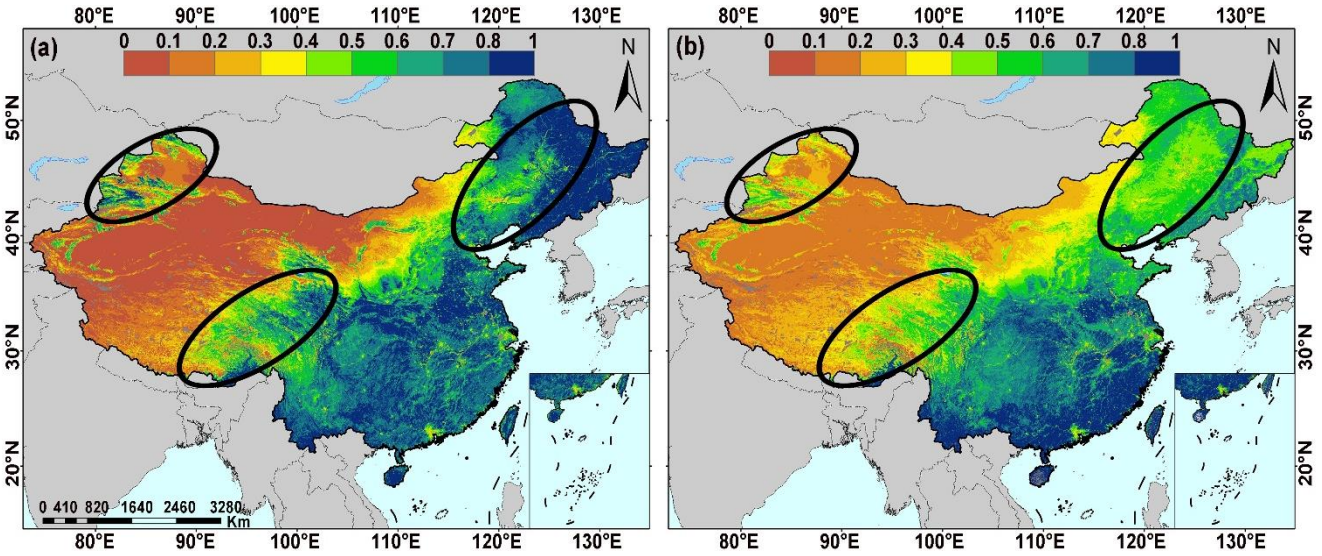

Figure 1. Spatial distribution of fractional vegetation cover based on (a) MVC and (b) SAM. The calculation of fractional vegetation cover is mainly carried out using normalization (Ding et al., 2016), in which the minimum and maximum values of EVI corresponding to the cumulative frequency of 1% and 99% are selected, respectively. The fractional vegetation cover is represented by 0 ~ 1. The black circles refer to regions with significant differences.

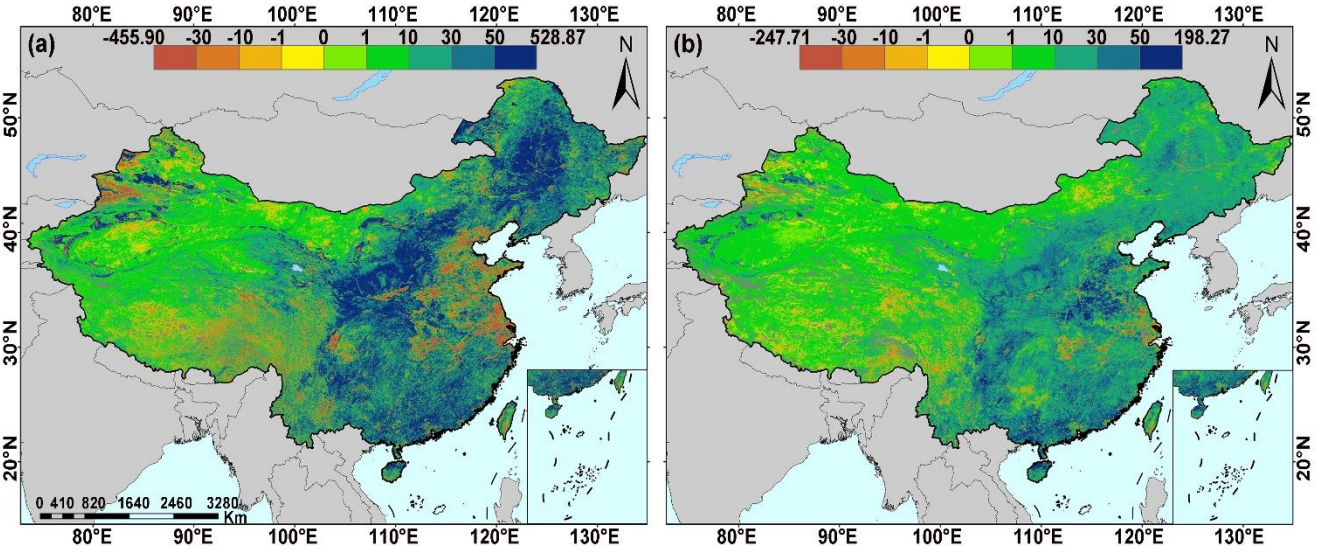

Figure 2. Greening rate and regional characteristics based on (a) MVC and (b) SAM.

the change of growing season length and type is relatively slight, and the change of maximum value can synergistically reflect the characteristics of EVI within the year (Compared with SAM, the regional greening trend after averaging is equally obvious, but it is weakened to a certain extent), which may be one of the essential factors that MVC is generally applicable to EVI characteristics (Figures 3d ~ 3f).

In some regions, it is not appropriate to characterize EVI changes by the maximum value. Regions 1 and 2 indicate the characteristic regions where the greening rate of EVI is less than −10/yr. Still, the browning region of MVC is improved in SAM, especially in region 1, whose EVI greening rate is greater than 50/yr. The reason is that the distribution of cultivated land and agricultural irrigation is mainly in region 1. The allometric growth of crops and the distribution coefficient of organ biomass have been changed due to the improvement of crop varieties and artificial adjustment. The proportion of organ biomass decreased, and more attention was paid to the proportion of yield-related fruit biomass, which led to a decrease in the maximum value but an increase in yield. At the same time, the adjustment of crop growing season is also the main factor causing the difference between MVC and SAM in Region 1. It is worth mentioning that this time point obtained by remote sensing data analysis with a resolution of 1 km is far behind the actual adjustment time of the planting structure in northern China (Figure 3b). Specifically, it may be that the actual area converted to mul-

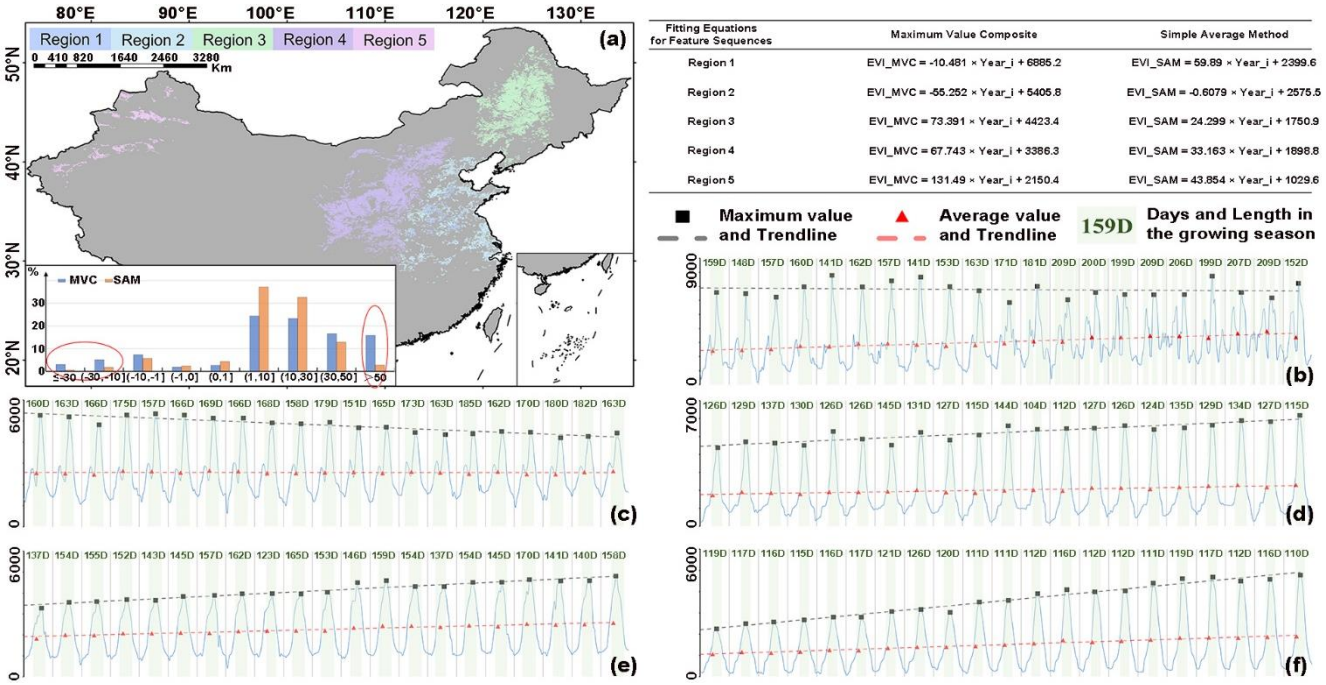

Figure 3. Selection of extreme regions and differences under methods. (a) The proportion of data and the distribution of extreme conditions under different greening rates, where the distribution of regions 1 ~ 5 is obtained by using the data difference in red circles. (b) ~ (f) The spatial average results of EVI in regions 1 ~ 5, where the abscissa is from 2001 to 2021, and the ordinate is dimensionless EVI data.

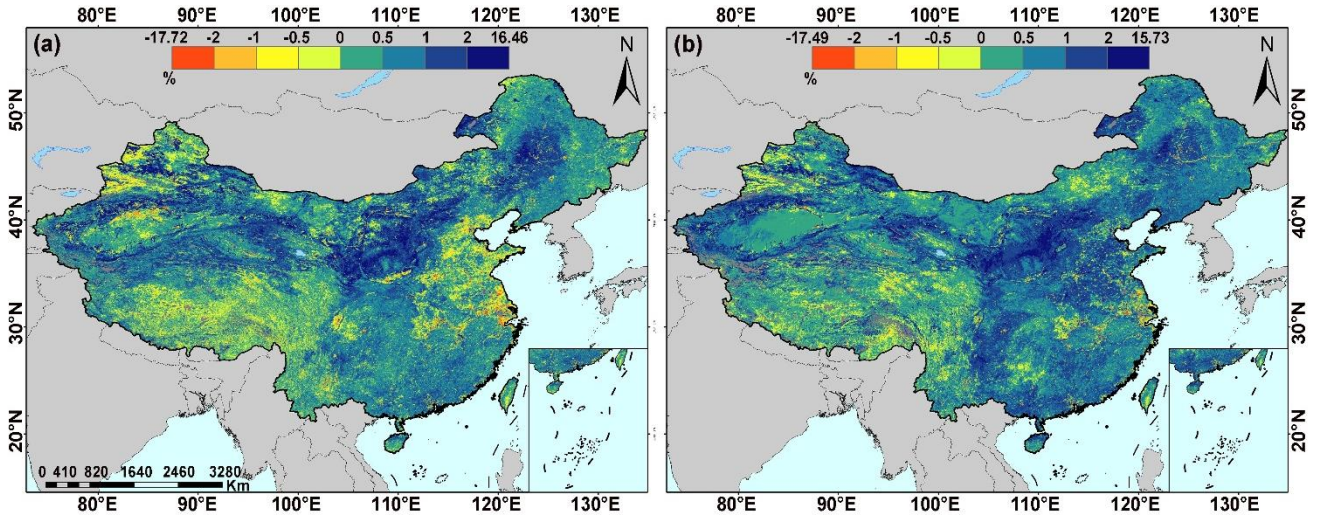

Figure 4. Greening degree and regional characteristics based on (a) MVC and (b) SAM.

tiple cropping in the region before 2011 is not enough to reflect in the 1km source data, and the research on crop phenology information needs to be supported by more detailed data. Region 2 is a complex area such as urban and agricultural land with a dense population and traffic, and the length and type of the regional growing season have not changed significantly. The regional maximum value has dropped significantly, but the average value trend is only −0.6079, which shows that although the MVC greening within the year has been lost to a certain extent in the human-influenced area, compensation has been made in the annual greening (Figure 3c). For some cultivated land, agricultural irrigation areas, and other areas affected by human-influenced, it is not entirely correct to reflect greening characteristics by using MVC, and the overall characteristics within the year need to be considered.

3.3. Difference of Greening Degree

The gradient change of the greening trend relative to its

average value of MVC (SAM) sequence in China was constructed (Figures 4a and 4b). Since 2013, the Chinese government has taken a series of measures, and the greening effect is equally remarkable (the greening degree improvement rate based on SAM: 196.90%. Greening degree improvement rate based on MVC: 226.44%). Considering the impact of artificial surfaces on the human footprint (Venter et al., 2016a; 2016b) in the 2010 GlobeLand 30 land cover data (Chen et al., 2017), more than 95th percentile is used to distinguish areas that are less and significantly affected by human activities, and then it is determined that the impact degree in the footprint needs to be no less than 10 (Figure 5a). While in the area less affected by human activities, we mainly explore the change of forest, grassland, shrubland, and wetland in land cover.

In the areas significantly affected by human activities, the MVC considering the annual maximum value shows that the frequency distribution of relative gradient mostly presents the trend of platykurtic, and the closer the relative gradient is to the extreme, the more pronounced the platykurtic situation of EVI trend distribution (Figure 5a: MVC-Group). It shows that the data is more random and disturbing when it is closer to the extreme case, which echoes the regional characteristics in Figure 3b. And this randomness and disturbance may make it more difficult for us to evaluate the greening degree. However, the SAM considering the annual homogenization information shows that

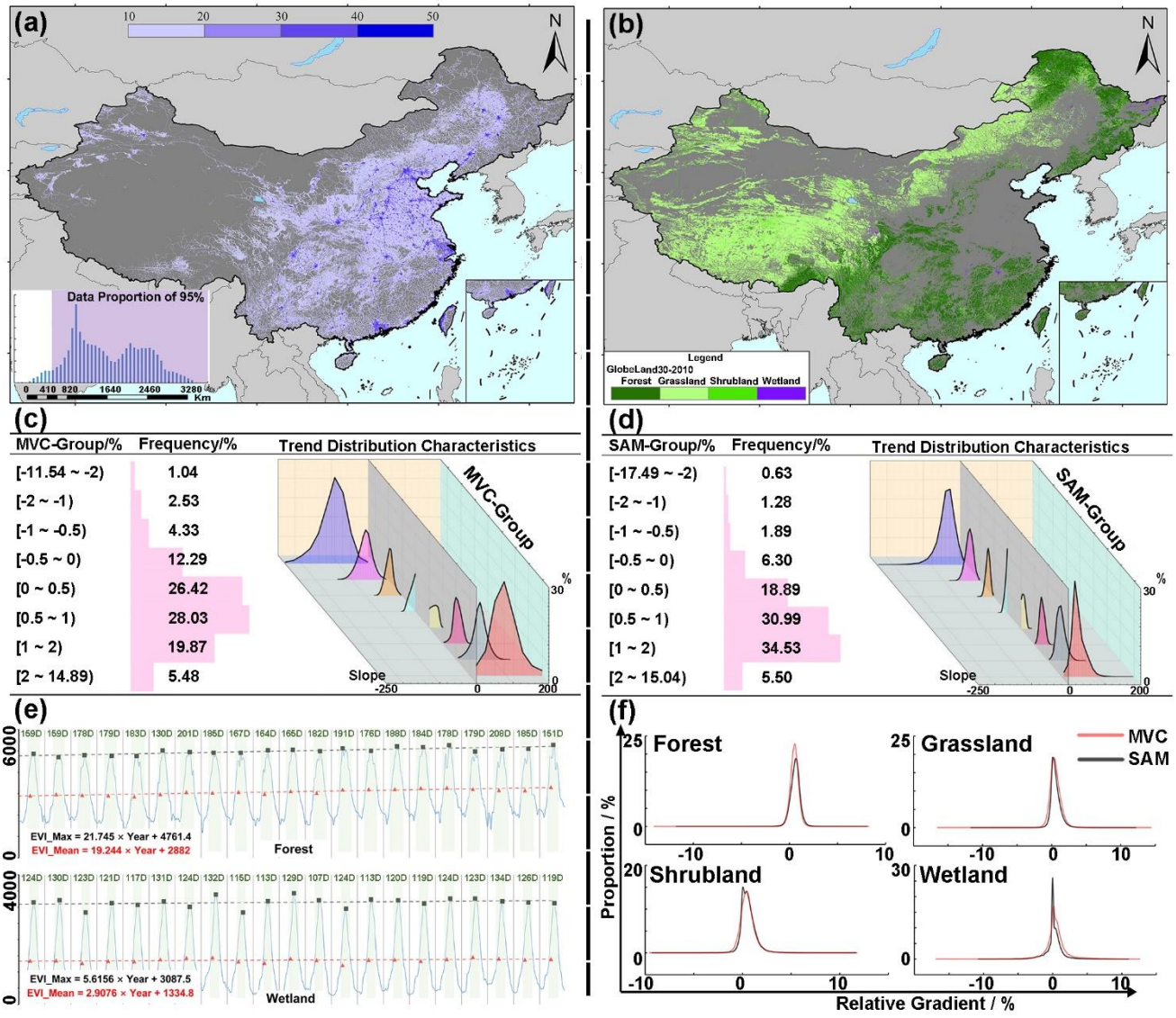

Figure 5. Sensitivity to Green degree. (a) Mainly includes the areas significantly affected by human activities and the characteristics of distribution and trend based on MVC and SAM. (b) Mainly includes spatial distribution of forest, grassland, shrubland and wetland in the area less affected by human activities, and the distribution characteristics of greening information and relative gradient. The abscissa of the forest and wetland is from 2001 to 2021, and the ordinate is the dimensionless EVI data. The human footprint data range is from 0 to 50, which belongs to dimensionless data.

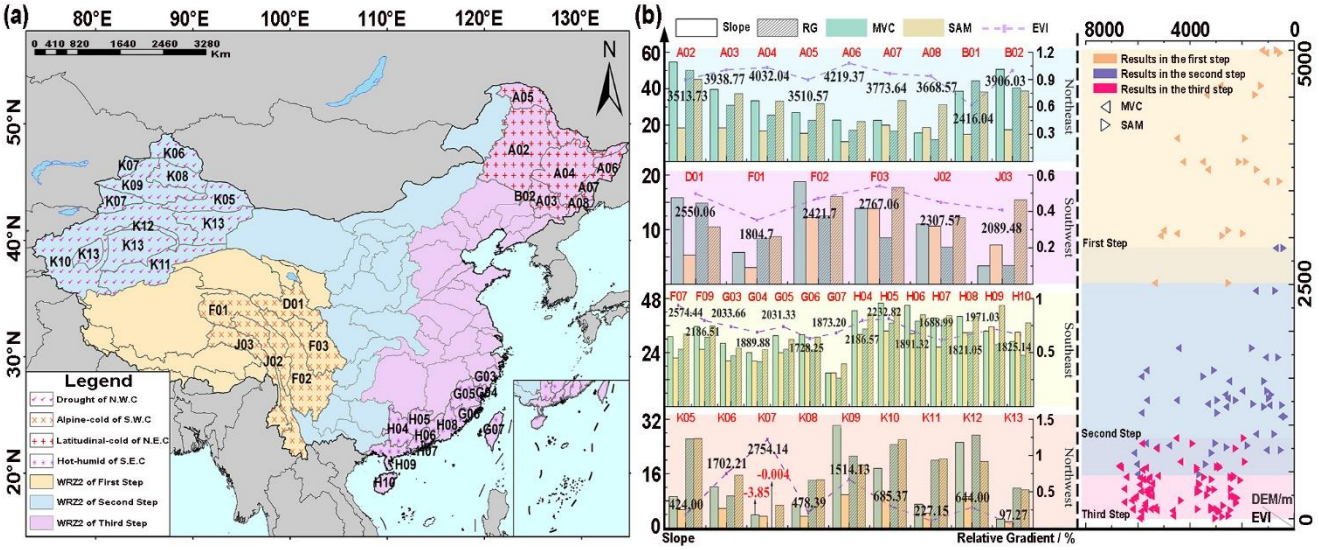

Figure 6. The WRZ2 based on three-step terrain and zoning characteristics. In the bar plot of subfigure (b), the red is used to represent different regions in the left subfigure, and the black is used to represent the average EVI of the regions.

the EVI shows the leptokurtic degree in both the frequency distribution of relative gradient and the trend change, which is relatively concentrated as a whole, reduces the disturbance influence of extreme conditions, and can accurately evaluate the change form of greening characteristics (Figure 5a: SAM-Group).

In the area less affected by human activities, the relative gradient distribution of forest, grassland, shrubland and wetland are relatively concentrated (Figure 5b). The contribution of forest to greening is the highest, mostly concentrated in 0.5812% (MVC) and 0.8065% (SAM). The second is grassland, mostly concentrated in 0.3349% (MVC) and 0.1200% (SAM). Then shrubland, mostly concentrated in 0.3530% (MVC), 0.0178% (SAM). The contribution of wetlands is the lowest, mostly concentrated on both sides of 0. As examples of forest and wetland with relatively high differentiation, the growing season length has not changed significantly. And the annual maximum value of vegetation in areas less affected by human activities has a greater influence on the EVI change, so we can choose to characterize the greening by the annual maximum value.

3.4. Difference and Identification of Greening Characters

Based on the terrain and geomorphology characteristics of China three-step terrain, we classify the two-level water resources zoning (WRZ2) in China (Figure 6). With the improvement of the terrain level, the EVI gap calculated by MVA and SAM will increase significantly, which is not only related to altitude, but also affected by many factors such as latitude zone and climatic conditions. Therefore, we mainly discuss the trend change and relative gradient difference in typical areas such as drought, alpine-cold, latitudinal-cold and hot-humid. Limited by the climate and drought, the vegetation growth conditions are harsh, the average vegetation coverage in northwest China is about 5.67% (statistics by SAM method), and the statistical difference of EVI within the region is relatively low. In the area less affected by human activities (Figure 5a and Figure 6: K05, K08, K11, K13 in Northwest), the EVI trend changes of maximum value and average value are relatively close to their relative gradient changes, and the greening rate is steadily and gradually promoted by 0.3757% (SAM) ~ 0.6436% (MVC) every decade. In the areas significantly affected by human activities, the greening rate is steadily and gradually promoted by 0.7604% (SAM) ~ 1.6232% (MVC) every decade, and the overall impact of human activities on vegetation greening is positive and obvious (Figure 5a and Figure 6: K06 ~ 07, K09 ~ 10 and K12 in Northwest).

Based on the two methods, the differences of vegetation coverage in the hot-humid of the southeast, the alpine-cold of the southwest, and the latitudinal-cold of northeast latitude are 19.95, 23.23, and 36.64%, respectively. And the average vegetation coverage in the region is about 36.48, 22.45, and 24.13% (SAM). Due to the relatively dominant vegetation growth conditions, the impact of human activities is averaged in largescale statistics, and no difference law is obtained. The trend of EVI obtained by MVC is higher than that by SAM, but the relative gradient is the opposite. Considering the change of annual Homogenized information in the region is more conducive to synergistically reflecting the contribution of vegetation greening degree. The greening rate in the three areas are 2.7084% (SAM) ~ 3.3743% (MVC), 0.8726% (SAM) ~ 1.1453% (MVC), 1.6774% (SAM) ~ 3.3863% (MVC) per decade, respectively.

According to the statistical differences between MVC and SAM, it can be concluded that (1) Except for drought areas, SAM is more suitable to characterize greening characteristics in the areas significantly affected by human activities. The impact of human activities is mostly positive, and due to poor vegetation growth conditions, the annual maximum value can basically reflect the year's overall characteristics. (2) MVC is more

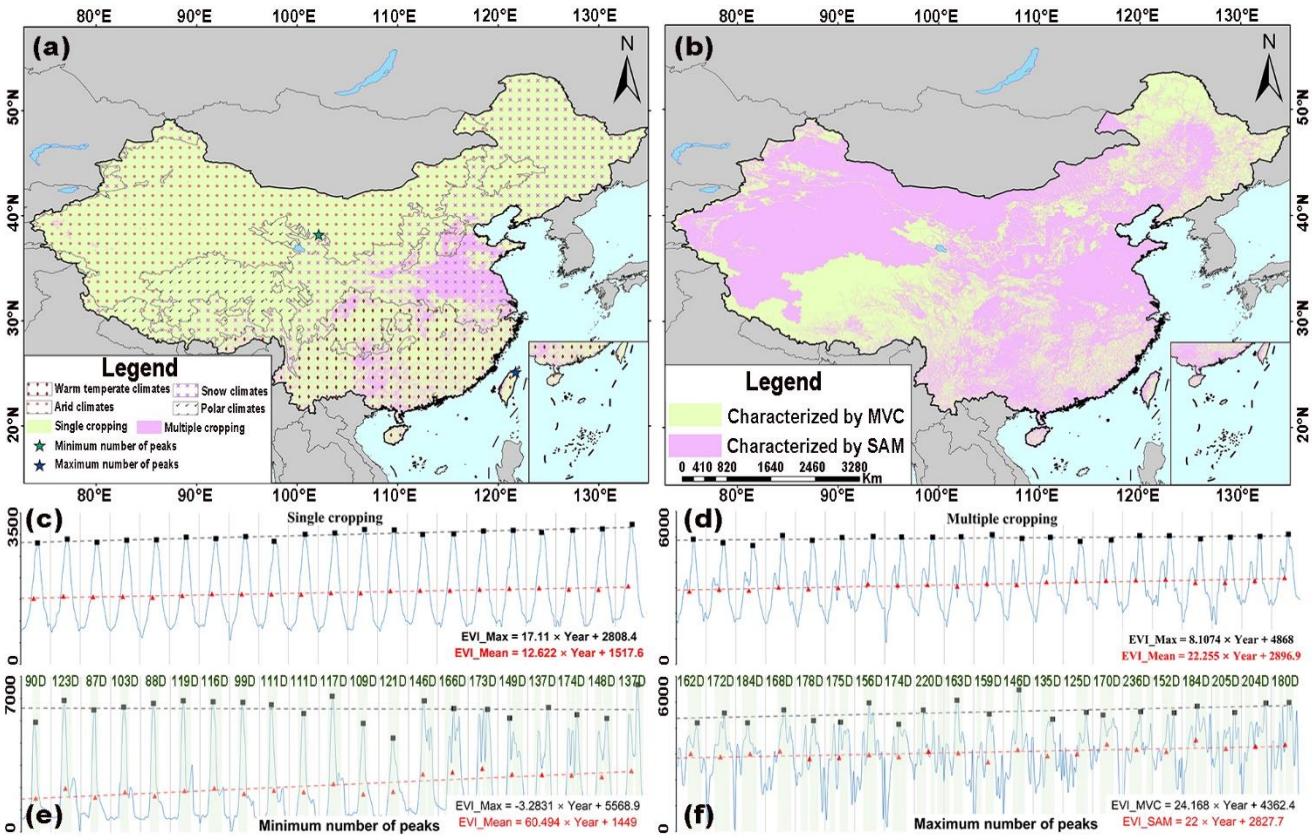

Figure 7. Identification and Integration Identification of greening characteristics. (a) Distribution of climate classification, single/multiple cropping, and minimum/maximum number of peaks. (b) Influence areas of MVC and SAM. (c) ~ (d) Greening information of single/multiple cropping. (e) ~ (f) Minimum/Maximum number of peaks in multiple cropping unit, where the abscissa is from 2001 to 2021, and the ordinate is dimensionless EVI data.

suitable to characterize greening characteristics in the area less affected by human activities. (3) The discrete Fourier transform function (Adole et al., 2018) is fitting on the EVI data processed by SG filtering (Arvor et al., 2008; Xu et al., 2021), the peak value after fitting is judged (Condition: the peak interval is 4, and the lowest peak value is greater than the annual average EVI), and the spatial distribution of multiple cropping vegetation/crops in China is obtained (Figure 7a). The variation of the minimum/maximum number of peaks in the multiple cropping vegetation/crops is extracted to ensure the single/multiple identification accuracy fully, and the delay effect of the single/multiple time point is also found (Figures 7e and 7f). Considering the statistical results of cultivated land and single/multiple cropping areas in Section 3.2 (Figures 3b and 3c), the greening characteristics of multiple cropping vegetation/crops are characterized by SAM, while MVC is the opposite. Finally, combined with Köppen climate classification (Kottek et al., 2006), single/multiple cropping, and human activity influence, the selection range of indicators in China region was obtained (Figure 7b). Since 2000, China has steadily and gradually promoted the greening rate of 1.73% every decade (Figure 8a). Compared with 2000 to 2013, the greening degree in China increased by 1.08 times (Figure 8b).

3.5. Contribution to Global Greening

We take the country as the statistical object to count the change degree of effective EVI cumulant in its region, discriminate the contribution degree of each region to global greening, and consider the change of contribution degree and the change in all information. Among them, the effective EVI value is not less than 0.

The number of countries with a greening trend dominates, and the global cumulative sequence of gaps has a significant upward trend compared with the slope between regions (Figure 9: Global_EVI). If only the contribution of regional cumulant to global change is considered, even if the greening range shows a downward or insignificant growth trend, the contribution degree will still be over-evaluated due to the influence of the magnitude of basic data (Table 2, Table 3, and Figure 9: Russia_EVI and USA_EVI). Taking complete account of the importance of greening degree and growth rate in the evaluation of regional greening contribution degree, we constructed a cumulative contribution comparison method considering the influence of slope (Equations 5 ~ 6). From 2001 to 2021, China, Brazil, India, and other countries made more active contributions to global greening, and the contribution degree is shown in Table 2. Brazil's greening rate is the fastest, which may be directly linked to hav-

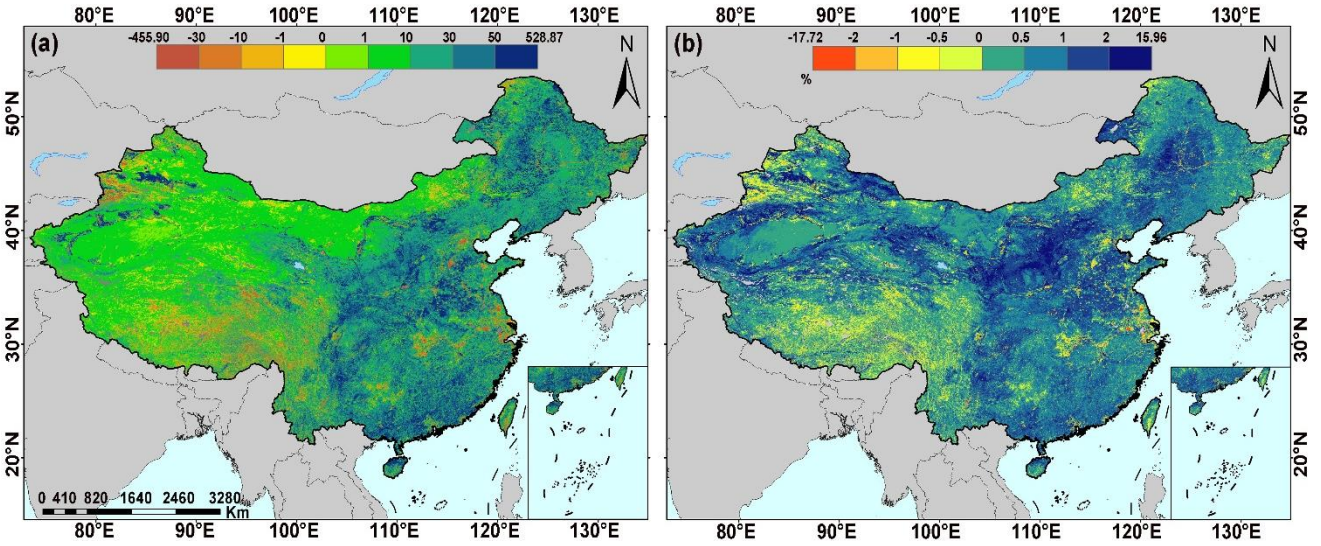

Figure 8. Identification and integration of greening characteristics: (a) Greening rate; (b) Greening degree.

Table 2. Ranking of Positive Changes to Greening During 2001 ~ 2021

Rank	Contribution of Cumulants		Contribution of Slope		Contribution under Combined Influence	
	Contribution	Nation	Contribution	Nation	Contribution	Nation
1	34.83	Russia	19.39	Brazil	13.72	China
2	22.10	U.S.A	15.27	China	10.40	Brazil
3	20.16	DR Congo	11.44	India	7.05	India
4	17.42	China	3.47	France	2.10	U.S.A
5	11.94	India	3.42	Poland	1.20	DR Congo
6	10.40	Brazil	3.27	Germany	1.13	Russia
7	4.90	Angola	2.99	Iran	0.50	Sudan
8	3.49	Namibia	2.85	Sudan	0.28	Pakistan
9	3.40	Sudan	2.83	Ukraine	0.24	Indonesia
10	3.02	Mongolia	2.56	Romania	0.22	Cote d'Ivoire

Table 3. Ranking of Negative Changes to Greening During 2001 ~ 2021

Rank	Contribution of Cumulants		Contribution of Slope		Contribution under Combined Influence	
	Contribution	Nation	Contribution	Nation	Contribution	Nation
1	−23.40	Australia	−13.05	Canada	−18.46	Canada
2	−18.46	Canada	−5.46	Peru	−1.83	Australia
3	−4.93	Tanzania	−3.31	Indonesia	−0.65	Germany
4	−4.88	Mozambique	−2.82	Zambia	−0.55	Ukraine
5	−3.86	Ukraine	−2.03	U.S.A	−0.19	Madagascar
6	−3.83	Madagascar	−1.87	Madagascar	−0.37	Poland
7	−3.83	Germany	−1.51	Argentina	−0.17	Mozambique
8	−2.82	Saudi Arabia	−1.01	Kazakhstan	−0.56	Tanzania
9	−2.41	Kazakhstan	−1.00	Mozambique	−0.32	Kazakhstan
10	−1.84	Poland	−0.65	Russia	−0.14	Saudi Arabia

ing most of the Amazon forest, but we believe in its unique positioning perspective as a big climate country (Viola and Franchini, 2017). In the dry season of the Amazon forest, which is not constrained by water, the increase in sunshine (Huete et al., 2006; Saleska et al., 2016) and the seasonality of water-use efficiency (Morton et al., 2014) may promote its greening trend. Also, Brazil's climate leadership is even more pronounced (Table 2) due to increased forest protection (Viola and Franchini, 2017). Brazil accounts for 5.71% of the global land area, and its cumulative contribution to global greening has reached10.40%.

Compared with Brazil, the cumulant sequence of gaps between China and India basically shows positive changes, and the greening is obvious. China has 6.44% of the global land area, and its cumulative contribution to global greening has reached

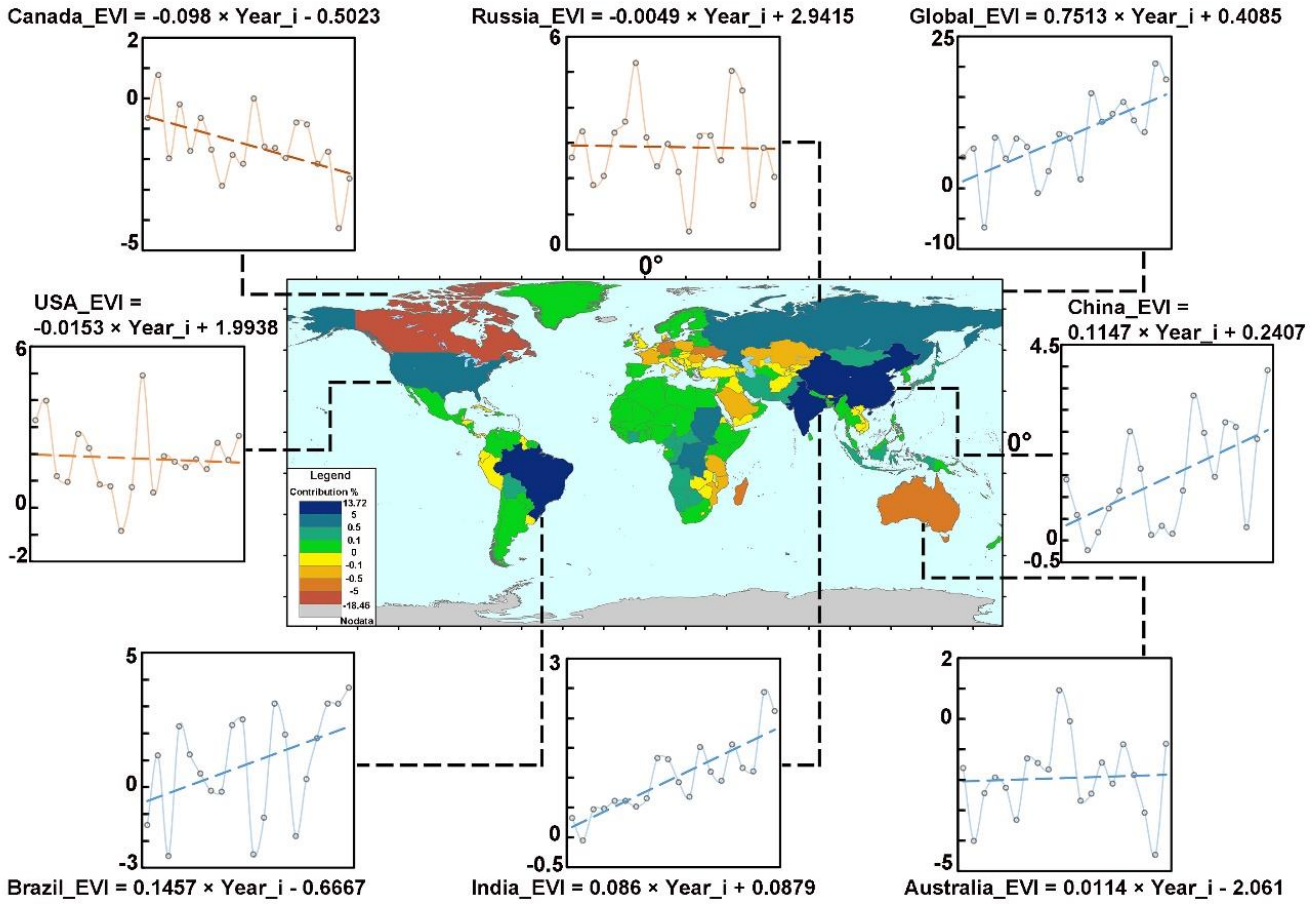

Figure 9. Contribution of regional greening. The solid line represents the trend of EVI change, the dashed line represents the fitted trend line, and its fitting equation can be obtained from the figure. Orange indicates a downward trend in the region, and blue indicates an upward trend. Notes: Because of the cumulant sequence of gaps, the abscissa is from 2002 to 2021, and the ordinate is the dimensionless cumulative EVI data (10^9).

13.72%. India has 2.00% of the global land area, and its cumulative contribution to global greening has reached 7.05%. The cultivated land of multiple cropping (Zuo et al., 2014) and Redlines for the greening (Lü et al., 2013) gives China a greater ability to achieve the goal of forest expansion, while India mainly focuses on farmland greening (Gao et al., 2019). The greening patterns of China and India are diametrically opposite, which are undoubtedly the two extremes of successful examples (Chen et al., 2019). However, the greening patterns of each region need to be fully considered according to regional characteristics and policy needs.

Canada is more prominent in the negative contribution of global greening (Table 3), and the cumulant sequence of gaps shows negative changes, which may be related to the higher value in 2001, but this is not enough to explain its significant downward trend (Figure 9: Canada_EVI). The browning of Canada has been discovered for a long time. At first, scholars speculated that this trend might be caused by many objective factors, such as the influence of processing algorithms, the difference in dataset pixels, etc (Alcaraz et al., 2010). However, based on the research about the combination of multi-source data sets (Beck and Goetz, 2011), productivity model (Zhang et al., 2008; Feng et al., 2021b), and the limiting factors of tree growth based on temperature (Lloyd et al., 2007; Man et al., 2013), water (Barber et al., 2004), insects (Malmström and Raffa, 2000), diseases (Malmström and Raffa, 2000), and other characteristics studies, many scholars have revealed in more detail the fact that the browning in northern North America is expanding. The vast land area and complex geographical environment in the region may be one of the reasons, but it is not the key. In the context of frequent global warming and extreme events, countries still need to pay attention to the degree of greening-browning transition at all times, especially in the northern region (Figure 9).

4. Discussion

4.1. A Single Index Cannot Characterize the Greening, and the Phenomenon of Hasty Generalization is more Prominent

China greening has achieved remarkable results and is almost common sense. Under such information's impact, the re-

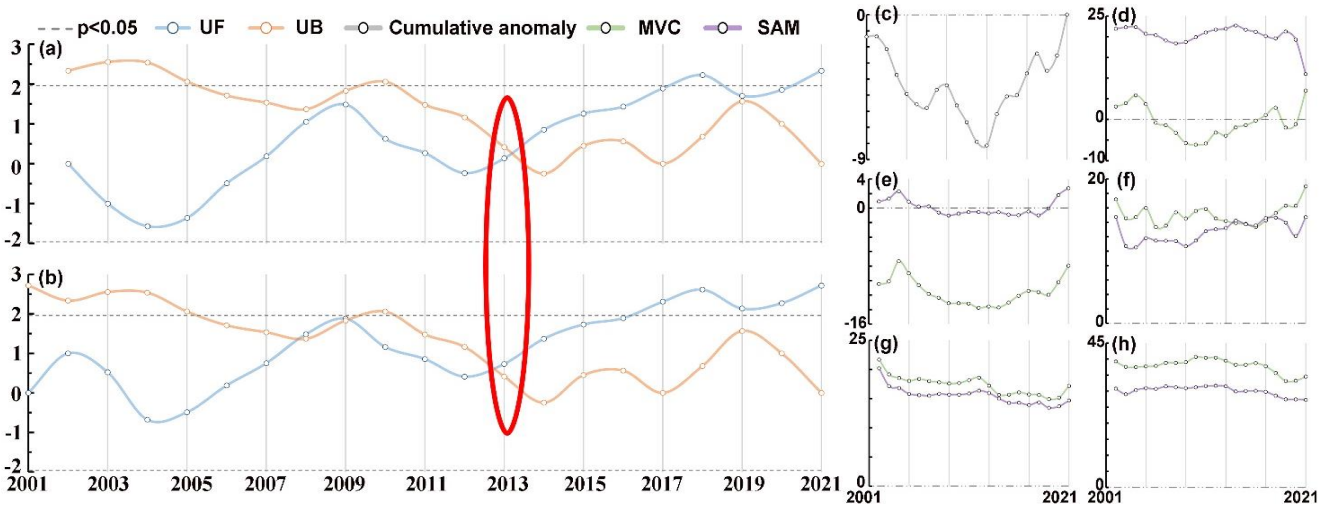

Figure 10. Comprehensive judgment of abrupt time point. (a) ~ (b) Results of the Mann-Kendall test and the moving t-test. (c) Results of the cumulative anomaly method. (d) ~ (h) The absolute error of the average value before and after the moving time (%), where the range of moving time is 2002 ~ 2021. Taking the moving time of 2002 as an example, this value is the absolute error of the average between 2001 and 2002 ~ 2021. Notes: The red circle highlights the turning point of the abrupt time.

search's focus is biased toward its driving factors, and the greening-browning boundary is easily ignored. Then the indexes that describe the greening trend are very critical. Different methods, such as selecting the maximum value (Yuan et al., 2022), statistical mean value (Pei et al., 2021), and statistical growth season changes in fixed months (Hua et al., 2017), have unique advantages. However, this have changed the greening-browning boundary to a certain extent, and the uncertainty of subsequent research results has also increased. Even with the most basic methods, the difference in greening-browning is still pronounced. The proportion of the area in which both are reversed is about 14.08%, far exceeding the proportion of the area where both brown together (6.66%) in China. The indicators that characterize greening are particularly complex in both spatial distribution and temporal evolution due to the influence of human activities, climate, and geographical environment. A single index of greening represents the overall characteristics, and there will be a phenomenon of hasty generalization. Due to the change in land type, the improvement of the agricultural model, and many other influences, the maximum value in the process of time evolution decreases, but the annual growing season and the overall greening trend show the opposite direction. And the above effects are also related to climate change. The above phenomena are also strongly related to climate change and differences in natural geographical environment. For example, in the drought of northwest China (Guan et al., 2018; Wu et al., 2021), the alpine-cold of southwest China (Liu et al., 2020; Qiao et al., 2021), and the latitudinal-cold of northeast China (Hua et al., 2017; Yuan et al., 2021), due to the limitation of water and temperature, the change of vegetation greening information in the annual distribution is not significant. It is worth mentioning that NDVI (de Jong et al., 2011; Zheng et al., 2015), LAI (Munier et al., 2018), and other greenness proxies used to characterize vegetation status are similar to the changes in EVI in this research. Selecting a fixed index in the trend analysis of discrete data will inevitably invert or attenuate the annual growing season of vegetation and the overall greening trend. The uncertainty of human influence, water, and temperature differences is still very complex in evolution, and this phenomenon of hasty generalization should be selectively recognized, considering the research's primary goal.

4.2. The Difference in China Greening Characteristics under 1 km Spatial Resolution is more Reflected around 2013. And the Forcing Facts of Extreme Regions 1 ~ 5 are Distinct under Different Methods

In this research, 2013 is often used as the time point when China greening characteristics changed significantly because the cumulation of quantitative changes leads to qualitative change. Through the Mann-Kendall test (Mann, 1945; Kendall, 1975), the moving t-test (Zhang et al., 2014), and the cumulative anomaly method (Zhao et al., 2015), it is confirmed that overall greening characteristics have an abrupt upward trend around 2013 (Figures 10a ~ 10c). And the regional changes in extreme cases are more sensitive, which the obvious changes around 2013 are very prominent and have different characteristics (Figures 10d ~ 10h). In regions 3 ~ 5, where vegetation growth is limited, the effects of different methods are almost the same, and the maximum value is more prominent. In regions with favorable vegetation growth, the variation differences are more complex. In region 1, which is dominated by cultivated land, the opposite trend is significant, and the average value can better highlight the volatility of its changes. In region 2 of complex types, the effects between different methods are also in the same trend, but the maximum value can better represent the fluctuation of changes. Specifically, this volatility or instability of changes is a more sensitive index that reflects the greening characteristics. It is worth mentioning that the point where the vegetation greening trend has changed significantly is closely

Table 4. Results of Partial Correlation Analysis

Methods	Statistical objectives		Region 1	Region 2	Region 3	Region 4	Region 5
MVC	SO1	p	0.0217	0.5428	0.1162	0.4791	0.0172
		R^2	−0.5097	−0.1447	0.3625	0.1680	0.5262
	SO2	p	0.7518	0.6624	0.2466	0.4554	0.0498
		R^2	0.0755	−0.1041	0.2717	−0.1770	0.4440
SAM	SO1	p	0.0393	0.9594	0.0007	0.0077	0.0957
		R^2	0.4641	−0.0122	0.6956	0.5773	0.3829
	SO2	p	0.0000	0.7556	0.0011	0.0000	0.0003
		R^2	0.8233	0.0743	0.6729	0.8119	0.7206

SO1: Considering the influence of temperature, the partial correlation between precipitation and vegetation. SO2: Considering the influence of precipitation, the partial correlation between temperature and vegetation. Reference: Song and Ma, 2011.

Table 5. Contribution Ratio of Slope

Methods	Statistical objectives		Region 1	Region 2	Region 3	Region 4	Region 5
MVC	Change ratio	SO3	35.8	−3.96	18.21	5.04	39.41
		SO4	1.34	−1.06	2.95	−1.03	2.51
		SO5	−4.76	−13.83	14.44	17.39	47.74
	Contribution ratio	SO3	−753.27	28.60	126.08	28.97	82.55
		SO4	−28.26	7.64	20.43	−5.91	5.25
		SO6	881.53	63.75	−46.52	76.94	12.20
SAM	Change ratio	SO3	2.29	10.82	16.31	11.85	15.33
		SO4	6.44	7.26	11.78	12.43	6.77
		SO5	24.11	−1.54	14.53	15.88	35.60
	Contribution ratio	SO3	9.51	−701.88	112.22	74.61	43.07
		SO4	26.70	−470.92	81.04	78.28	19.01
		SO6	63.79	1272.79	−93.26	−52.89	37.92

SO3: Precipitation. SO4: Temperature. SO5: EVI. SO6: Other factors, such as human activities. The change and Contribution ratio are obtained by the slope change ratio of accumulative quantity (Wang et al., 2012; Wu et al., 2017).

related to the resolution of the source data. Taking Region 1 as an example, when analyzing the 500 m source data, the time of the double-peak is earlier.

We further analyze the influencing factors based on the change in precipitation and temperature (Tables 4 and 5). The positive relationship between the precipitation and the vegetation greening is generally promoting, and the temperature increase has more influence on agricultural changes such as crop type and rotation. The planting structure in region 1 has changed significantly during the year. The difference between MVC and SAM methods in partial correlation analysis is more reflected in temperature evolution. And in considering the overall vegetation information in the region, the contribution of temperature and other factors, such as human activities, is pronounced. The land pattern in region 2 is more complex, with many types of urban and agricultural land with dense population and traffic. The greening of the vegetation landscape pattern is dominant, and the double-peaks are not evident during the year. The partial correlation results in complex types of combination regions are insignificant, and the contribution of other factors, such as human activities, is obviously dominant. Regions 3 and 4 both show that the partial correlation analysis results of SAM considering the overall greening information are significant, and MVC is the opposite. We conjecture that this result is related to the effective annual changes of precipitation and temperature in the month with the maximum value, and recombined sequences have low representation. The dominant factors affecting its trend change are more reflected in climate change. Region 5 is affected by the environment, and the annual vegetation information is more reflected in the maximum value. Compared with the partial correlation analysis results of MVC, SAM is relatively insignificant. The dominant factors are more reflected in precipitation and other factors, such as human activities.

5. Conclusions

Few papers discuss greening reflected in method differences. The description of the greening phenomenon by the choice of statistical indicators may only be a high and low change in the overall statistics, but there may be directional errors and the phenomenon of hasty generalization in some regions. This difference is obviously not desirable in the analysis of driving factors and their contribution. In this research, the statistical indicators constructed by MVC and SAM evaluated the method differences in China greening characteristics from the greening rate and degree perspective, and revealed the occurrence and characteristics of this difference. Vegetation growth conditions and variation characteristics during the year have the highest priority in greening. In regions with limited vegetation growth conditions, such as northwest and northeast China, the annual maximum value can synergistically reflect the annual greening characteristics, highlighting its significant trend. In regions of cultivated land that are more profitable by changing crop characteristics during the year, the annual maximum value cannot accurately distinguish the range of greening-browning, and the SAM method that considers the annual information performs better.

Ignoring the case of multiple cropping, the influence of human activities is mostly positive in the annual information, and SAM is more suitable to characterize its greening characteristics.

Under the background of global greening, the quantitative contribution of different regions has not been thoroughly studied. The contribution of greening should fully consider the vegetation cover characteristics of inherent stock and changing flux. By analyzing the cumulant sequence of gaps, we show that China has accounted for 6.44% of the global land area and contributed 13.72% to global greening, ranking first. Brazil (10.40%), followed by India (7.05%). The browning phenomenon in Canada is remarkable, and the accompanying problems, such as ecosystem sustainability and species diversity, need to be paid enough attention.

Appendix

Table A1. The Code and Corresponding Name of WRZ2

Code	Name
A02	Nenjiang river
A03	Di'er Songhua river
A04	Songhua River (below the Sanchakou)
A05	Main stream of Heilongjiang river
A06	Wusuli River
A07	Suifen river
A08	Tumen River
B01	Xiliao River
B02	Dongliao River
D01	Yellow River above Longyang Gorge dams
F01	Jinsha River above shigu
F02	Jinsha River under shigu
F03	Mintuo River
J02	Lancang River
J03	Nujiang River and Irrawaddy River
F07	Dongting Lake water system
F09	Poyang Lake water system
G03	Rivers in southern Zhejiang
G04	Rivers in eastern Fujian
B01	Xiliao River
B02	Dongliao River
D01	Yellow River above Longyang Gorge dams
F01	Jinsha River above shigu
F02	Jinsha River under shigu
F03	Mintuo River
J02	Lancang River
J03	Nujiang River and Irrawaddy River
F07	Dongting Lake water system
F09	Poyang Lake water system
G03	Rivers in southern Zhejiang
G04	Rivers in eastern Fujian
G05	Minjiang river
G06	Rivers in southern Fujian
G07	Rivers in Taiwan
H04	The Xijiang River of the Pearl River
H05	The Beijiang River of the Pearl River
H06	The Dongjiang River of the Pearl River
H07	Zhujiang delta
H08	Hanjiang River and rivers in eastern Guangdong
H09	Rivers in western Guangdong and southern Guangxi
H10	Hainan Island and South China Sea Islands
K05	Rivers in Turpan-Hami Basin
K06	Rivers at the southern foot of Altai Mountain
K07	Inland river region of Central Asia and West Asia
K08	Gurbantunggut Desert Area
K09	Rivers at the northern foot of Tianshan Mountain
K10	Source of Tarim River
K11	Rivers at the north foot of Kunlun Mountain
K12	Main stream of Tarim River
K13	Desert area of Tarim Basin

Acknowledgments. The researchers would like to extend their thanks to the National Science Fund Project for Distinguished Young Scholars (Grant No. 51725905), and the National Science Fund Project (Grant No. 52130907).

References

Aubinet, M., Vesala, T. and Papale, D. (2012). *Eddy covariance: A practical guide to measurement and data analysis*. Springer Dordrecht, pp 1-438. https://doi.org/10.1007/978-94-007-2351-1

Adole, T., Dash, J. and Atkinson, P.M. (2018). Characterising the land surface phenology of Africa using 500 m MODIS EVI. *Appl. Geogr.*, 90, 187-199. https://doi.org/10.1016/j.apgeog.2017.12.006

Alcaraz-Segura, D., Chuvieco, E., Epstein, H.E., Kasischke, E.S. and Trishchenko, A. (2010). Debating the greening vs. browning of the North American boreal forest: differences between satellite datasets. *Global Change Biol.*, 16(2), 760-770. https://doi.org/10.1111/j.1365-2486.2009.01956.x

Arvor, D., Meirelles, M.S.P., Dubreuil, V. and Lecerf, R. (2008). Comparison of multitemporal MODIS-EVI smoothing algorithms and its contribution to crop monitoring. *In IGARSS 2008-2008 IEEE International Geoscience and Remote Sensing Symposium*, 2, II-958-II-961. https://doi.org/10.1109/IGARSS.2008.4779155

Barber, V.A., Juday, G.P. and Finney, B.P. (2004). Reconstruction of summer temperatures in interior Alaska from tree-ring proxies: evidence for changing synoptic climate regimes. *Clim. Change*, 63(1), 91-120. https://doi.org/10.1023/B:CLIM.0000018501.98266.55

Beck, P.S.A. and Goetz, S.J. (2011). Satellite observations of high northern latitude vegetation productivity changes between 1982 and 2008: ecological variability and regional differences. *Environ. Res. Lett.*, 6(4), 045501. https://doi.org/10.1088/1748-3182/6/4/049501

Bogaert, J., Zhou, L., Tucker, C.J., Myneni, R.B. and Ceulemans, R. (2002). Evidence for a persistent and extensive greening trend in Eurasia inferred from satellite vegetation index data. *J. Geophys. Res-Atmos.*, 107(D11), ACL-4. https://doi.org/10.1029/2001JD001075

Chen, A., Lantz, T.C., Hermosilla, T. and Wulder, M.A. (2021). Biophysical controls of increased tundra productivity in the western Canadian Arctic. *Remote Sens. Environ.*, 258, 112358. https://doi.org/10.1016/j.rse.2021.112358

Chen, C., Park, T., Wang, X., Piao, S., Xu, B., Chaturvedi, R.K., Fuchs, R., Brovkin, V., Ciais, P., Fensholt, R., Tømmervik, H., Bala, G., Zhu, Z., Nemani, R.R. and Myneni, R.B. (2019). China and India lead in greening of the world through land-use management. *Nat. Sustain.*, 2(2), 122-129. https://doi.org/10.1038/s41893-019-0220-7

Chen, J., Cao, X., Peng, S. and Ren, H. (2017). Analysis and applications of GlobeLand30: a review. *ISPRS Int. J. Geo-Inf.*, 6(8), 230. https://doi.org/10.3390/ijgi6080230

Cortés, J., Mahecha, M.D., Reichstein, M., Myneni, R.B. and Brenning,

A. (2021). Where are global vegetation greening and browning trends significant? *Geophys. Res. Lett.*, 48(6), e2020GL091496. https://doi.org/10.1029/2020GL091496

de Jong, R., de Bruin, S., de Wit, A., Schaepman, M.E. and Dent, D.L. (2011). Analysis of monotonic greening and browning trends from global NDVI time-series. *Remote Sens. Environ.*, 115(2), 692-702. https://doi.org/10.1016/j.rse.2010.10.011

Ding, Y., Zheng, X., Zhao, K., Xin, X. and Liu, H. (2016). Quantifying the impact of NDVIsoil determination methods and NDVIsoil variability on the estimation of fractional vegetation cover in Northeast China. *Remote Sens-basel.*, 8(1), 29. https://doi.org/10.3390/rs8010029

Feng, D., Bao, W., Yang, Y. and Fu, M. (2021a). How do government policies promote greening? Evidence from China. *Land Use Policy*, 104, 105389. https://doi.org/10.1016/j.landusepol.2021.105389

Feng, X., Fu, B., Zhang, Y., Pan, N., Zeng, Z., Tian, H., Lyu, Y., Chen, Y., Ciais, P., Wang, Y., Zhang, L., Cheng, L., Maestre, F.T., Fernández-Martínez, M., Sardans, J. and Peñuelas, J. (2021b). Recent leveling off of vegetation greenness and primary production reveals the increasing soil water limitations on the greening Earth. *Sci. Bull.*, 66(14), 1462-1471. https://doi.org/10.1016/j.scib.2021.02.023

Forzieri, G., Alkama, R., Miralles, D.G. and Cescatti, A. (2017). Satellites reveal contrasting responses of regional climate to the widespread greening of Earth. *Science*, 356(6343), 1180-1184. https://doi.org/10.1126/science.aal1727

Gao, X., Liang, S. and He, B. (2019). Detected global agricultural greening from satellite data. *Agr. Forest Meteorol.*, 276-277(2), 107652. https://doi.org/10.1016/j.agrformet.2019.107652

Guan, Q., Yang, L., Pan, N., Lin, J., Xu, C., Wang, F. and Liu, Z. (2018). Greening and browning of the Hexi Corridor in northwest China: Spatial patterns and responses to climatic variability and anthropogenic drivers. *Remote Sens-basel.*, 10(8), 1270. https://doi.org/10.3390/rs10081270

Hua, W., Chen H., Zhou, L., Xie, Z., Qin, M., Li, X., Ma, H., Huang, Q. and Sun, S. (2017). Observational quantification of climatic and human influences on vegetation greening in China. *Remote Sens-basel.*, 9(5), 425. https://doi.org/10.3390/rs9050425

Huete, A.R., Didan, K., Shimabukuro, Y.E., Ratana, P., Saleska, S.R., Hutyra, L.R., Yang, W., Nemani, RR. and Myneni, R. (2006). Amazon rainforests green-up with sunlight in dry season. *Geophys. Res. Lett.*, 33(6), L06405. https://doi.org/10.1029/2005GL025583

Huete, A., Didan, K., Miura, T., Rodriguez, E.P., Gao, X. and Ferreira, L.G. (2002). Overview of the radiometric and biophysical performance of the MODIS vegetation indices. *Remote Sens. Environ.*, 83(1-2), 195-213. https://doi.org/10.1016/S0034-4257(02)00096-2

Kendall, M.G. (1975). *Rank correlation methods.* 4th Edition. Griffin, London, p1-202. https://www.researchgate.net/publication/264959683_Rank_Correlation_Methods

Kottek, M., Grieser, J., Beck, C., Rudolf, B. and Rubel, F. (2006). World map of the Köppen-Geiger climate classification updated. *Meteorol. Z.*, 15(3), 259-263. https://doi.org/10.1127/0941-2948/2006/0130

Liu, H., Jiao, F., Yin, J., Li, T., Gong, H., Wang, Z. and Lin, Z. (2020). Nonlinear relationship of vegetation greening with nature and human factors and its forecast-a case study of Southwest China. *Ecol. Indic.*, 111, 106009. https://doi.org/10.1016/j.ecolind.2019.106009

Liu, Y., Li, Y., Li, S. and Motesharrei, S. (2015). Spatial and temporal patterns of global NDVI trends: correlations with climate and human factors. *Remote Sens-basel.*, 7(10), 13233-13250. https://doi.org/10.3390/rs71013233

Lloyd, A.H. and Bunn, A.G. (2007). Responses of the circumpolar boreal forest to 20th century climate variability. *Environ. Res. Lett.*, 2(4), 045013. https://doi.org/10.1088/1748-9326/2/4/045013

Lü, Y., Ma, Z., Zhang, L., Fu, B. and Gao, G. (2013). Redlines for the greening of China. *Environ. Sci. Policy*, 33, 346-353. https://doi.org/10.1016/j.envsci.2013.05.007

Maina, F.Z., Kumar, S.V., Albergel, C. and Mahanama, S.P. (2022). Warming, increase in precipitation, and irrigation enhance greening in High Mountain Asia. *Commun. Earth Environ.*, 3(1), 1-8. https://doi.org/10.1038/s43247-022-00374-0

Malmström, C.M. and Raffa, K.F. (2000). Biotic disturbance agents in the boreal forest: considerations for vegetation change models. *Global Change Biol.*, 6(S1), 35-48. https://doi.org/10.1046/j.1365-2486.2000.06012.x

Mann, H.B. (1945). Nonparametric tests against trend. *Econometrica*, 13(3), 245-259. https://doi.org/10.2307/1907187

Man, R., Kayahara, G.J., Foley, S. and Wiseman, C. (2013). Survival and growth of eastern larch, balsam fir, and black spruce six years after winter browning in northeastern Ontario, Canada. *Forest. Chron.*, 89(6), 777-782. https://doi.org/10.5558/tfc2013-140

Morton, D.C., Nagol, J., Carabajal, C.C., Rosette, J., Palace, M., Cook, B.D., Vermote, E.F., Harding, D.J. and North, P.R.J. (2014). Amazon forests maintain consistent canopy structure and greenness during the dry season. *Nature*, 506(7487), 221-224. https://doi.org/10.1038/nature13006

Munier, S., Carrer, D., Planque, C., Camacho, F., Albergel, C. and Calvet, J.C. (2018). Satellite leaf area index: global scale analysis of the tendencies per vegetation type over the last 17 years. *Remote Sens-basel.*, 10(3), 424. https://doi.org/10.3390/rs10030424

Pei, H., Liu, M., Jia, Y., Zhang, H., Li, Y. and Xiao, Y. (2021). The trend of vegetation greening and its drivers in the Agro-pastoral ecotone of northern China, 2000-2020. *Ecol. Indic.*, 129, 108004. https://doi.org/10.1016/j.ecolind.2021.108004

Parida, B.R., Pandey, A.C. and Patel, N.R. (2020). Greening and browning trends of vegetation in India and their responses to climatic and non-climatic drivers. *Climate*, 8(8), 92. https://doi.org/10.3390/cli8080092

Piao, S., Wang, X., Ciais, P., Zhu, B., Wang, T. and Liu, J. (2011). Changes in satellite-derived vegetation growth trend in temperate and boreal Eurasia from 1982 to 2006. *Global Change Biol.*, 17(10), 3228-3239. https://doi.org/10.1111/j.1365-2486.2011.02419.x

Piao, S., Wang, X., Park, T., Chen, C., Lian, X., He, Y., Bjerke, J.W., Chen, A., Ciais, P., Tømmervik, H., Nemani, R.R. and Myneni, R.B. (2020). Characteristics, drivers and feedbacks of global greening. *Nat. Rev. Earth Env.*, 1(1), 14-27. https://doi.org/10.1038/s43017-019-0001-x

Propastin, P.A., Kappas, M. and Muratova, N.R. (2008). Inter-annual changes in vegetation activities and their relationship to temperature and precipitation in central asia from 1982 to 2003. *J. Environ. Inform.*, 12(2), 75-87. https://doi.org/10.3808/jei.200800126

Qiao, Y., Jiang, Y. and Zhang, C. (2021). Contribution of karst ecological restoration engineering to vegetation greening in southwest China during recent decade. *Ecol. Indic.*, 121, 107081. https://doi.org/10.1016/j.ecolind.2020.107081

Saleska, S.R., Wu, J., Guan, K., Araujo, A.C., Huete, A., Nobre, A.D. and Restrepo-Coupe, N. (2016). Dry-season greening of Amazon forests. *Nature*, 531(7594), E4-E5. https://doi.org/10.1038/nature16457

Song, Y. and Ma, M. (2011). A statistical analysis of the relationship between climatic factors and the Normalized Difference Vegetation Index in China. *Int. J. Remote Sens.*, 32(14), 3947-3965. https://doi.org/10.1080/01431161003801336

Venter, O., Sanderson, E.W., Magrach, A., Allan, J.R., Beher, J., Jones, K.R., Possingham, H.P., Laurance, W.F., Wood, P., Fekete, B.M., Levy, M.A. and Watson, J.E.M. (2016a). Global terrestrial Human Footprint maps for 1993 and 2009. *Sci. Data*, 3(1), 1-10. https://doi.org/10.1038/sdata.2016.67

Venter, O., Sanderson, E.W., Magrach, A., Allan, J.R., Beher, J., Jones, K.R., Possingham, H.P., Laurance, W.F., Wood, P., Fekete, B.M., Levy, M.A. and Watson, J.E.M. (2016b). Sixteen years of change in the global terrestrial human footprint and implications for biodiver-

sity conservation. *Nat. Commun.*, 7, 12558. https://doi.org/10.1038/ncomms12558

Viola, E. and Franchini, M. (2017). *Brazil and climate change: beyond the Amazon*. Routledge. https://doi.org/10.4324/9781315101651

Wang, S., Yan, Y., Yan, M. and Zhao, X. (2012). Quantitative estimation of the impact of precipitation and human activities on runoff change of the Huangfuchuan River Basin. *J. Geogr. Sci.*, 22(5), 906-918. https://doi.org/10.1007/s11442-012-0972-8

Wu, L., Wang, S., Bai, X., Luo, W., Tian, Y., Zeng, C., Luo, G. and He, S. (2017). Quantitative assessment of the impacts of climate change and human activities on runoff change in a typical karst watershed, SW China. *Sci. Total Environ.*, 601-602, 1449-1465. https://doi.org/10.1016/j.scitotenv.2017.05.288

Wu, Z., Bi, J. and Gao, Y. (2021). Drivers and environmental impacts of vegetation greening in a semi-arid region of northwest China since 2000. *Remote Sens-basel.*, 13(21), 4246. https://doi.org/10.3390/rs13214246

Xu, C., Zhang, X., Zhang, J., Chen, Y., Yami, T.L. and Hong, Y. (2021). Estimation of crop water requirement based on planting structure extraction from multi-temporal MODIS EVI. *Water Resour. Manag.*, 35(7), 2231-2247. https://doi.org/10.1007/s11269-021-02838-y

Yao, R., Wang, L., Huang, X., Chen, X. and Liu, Z. (2019). Increased spatial heterogeneity in vegetation greenness due to vegetation greening in mainland China. *Ecol, Indic.*, 99, 240-250. https://doi.org/10.1016/j.ecolind.2018.12.039

Yuan, W., Wu, S.Y., Hou, S. and Xu, Z. (2021). Projecting future vegetation change for northeast China using CMIP6 model. *Remote Sens-basel.*, 13(17), 3531. https://doi.org/10.3390/rs13173531

Yuan, Z., Xu, J.J., Chen, J., Wang, Y.Q. and Yin, J. (2022). EVI Indicated spatial-temporal variations in vegetation and their responses to climatic and anthropogenic factors in the chinese mainland since 2000s. *J. Environ. Inform.*, 40(2), 157-175. https://doi.org/10.3808/jei.202100467

Zhang, C., Zhang, B., Li, W. and Liu, M. (2014). Response of streamflow to climate change and human activity in Xitiaoxi river basin in China. *Hydrol. Processes*, 28(1), 43-50. https://doi.org/10.1002/hyp.9539

Zhang, K., Kimball, J.S. and Hogg, E.H., (2008). Satellite-based model detection of recent climate-driven changes in northern high-latitude vegetation productivity. *J. Geophys. Res-Biogeo.*, 113(G3), G03033. https://doi.org/10.1029/2007JG000621

Zhang, X., Friedl, M.A., Schaaf, C.B., Strahler, A.H., Hodges, J.C.F., Gao, F., Reed, B.C. and Huete, A. (2003). Monitoring vegetation phenology using MODIS. *Remote Sens. Environ.*, 84(3), 471-475. https://doi.org/10.1016/S0034-4257(02)00135-9

Zhao, Y., Zou, X., Gao, J., Xu, X., Wang, C., Tang, D., Wang, T. and Wu, X. (2015). Quantifying the anthropogenic and climatic contributions to changes in water discharge and sediment load into the sea: A case study of the Yangtze River, China. *Sci. Total Environ.*, 536, 803-812. https://doi.org/10.1016/j.scitotenv.2015.07.119

Zheng, B., Myint, S.W., Thenkabail, P.S and Aggarwal, R.M. (2015). A support vector machine to identify irrigated crop types using time-series Landsat NDVI data. *Int. J. Appl. Earth Obs.*, 34, 103-112. https://doi.org/10.1016/j.jag.2014.07.002

Zhu, Z., Piao, S., Myneni, R.B., Huang, M., Zeng, Z., Canadell, J.G., Ciais, P., Sitch, S., Friedlingstein, P., Arneth, A., Cao, C., Cheng, L., Kato, E., Koven, C., Li, Y., Lian, X., Liu, Y., Liu, R., Mao, J., Pan, Y., Peng, S., Peñuelas, J., Poulter, B., Pugh, T.A.M., Stocker, B.D., Viovy, N., Wang, X., Wang, Y., Xiao, Z., Yang, H., Zaehle, S. and Zeng, N. (2016). Greening of the Earth and its drivers. *Nat. Clim. Change*, 6(8), 791-795. https://doi.org/10.1038/nclimate3004

Zuo, L., Wang, X., Zhang, Z., Zhao, X., Liu, F., Yi, L. and Liu, B. (2014). Developing grain production policy in terms of multiple cropping systems in China. *Land Use Policy*, 40, 140-146. https://doi.org/10.1016/j.landusepol.2013.09.014